Shot Peening and Ball-Burnishing to Improve HCF Strength of the New Titanium Alloy TIMETAL-54M

K. Zay[1], Y. Shan[1], Y. Kosaka[2], L. Wagner[1]

[1] Institute of Materials Science and Engineering
Clausthal University of Technology
Clausthal-Zellerfeld
Germany

[2] Henderson Technical Laboratory
TIMET, Henderson, NV
USA

Abstract
TIMETAL-54M (Ti-5Al-4V-0.6Mo-0.5Fe) is a new (α+β) titanium alloy which was developed by TIMET, Henderson, NV (USA). The addition of small amounts of the β-stabilizers Mo and Fe and the reduction in Al-content reduce the β-transus temperature relative to Ti-6Al-4V and offer improved formability due to lower working temperatures and working stresses as well as better machinability (increased cutting speed and/or improved cutting tool life). Thus, TIMETAL-54M is supposed to provide a cost benefit for parts that require extensive machining.
Shot peening (SP) and ball-burnishing (BB) were performed on various well defined microstructures (fully equiaxed, fully lamellar, duplex) using a wide variation in process parameters to study potential improvements in HCF performance. The shot peening and ball-burnishing-induced changes in the surface and near-surface properties were evaluated by measurements of surface topography, micro-hardness-depth profiles and residual stress-depth profiles. The results indicate a marked influence of the microstructure on the observed HCF strength enhancements.

Keywords: TIMETAL-54M, HCF performance, shot peening, ball-burnishing.

Introduction

The most common titanium alloy is Ti-6Al-4V, which accounts for more than 50% of titanium alloy production. Recently, TIMET has developed an alloy called TIMETAL-54M (Ti-54M), which provides improved machinability and formability [1, 2]. The alloy with nominal composition (Ti-5Al-4V-0.5Mo-0.4Fe) is produced through Electron Beam Single Melt Process (EBSM) as the alloy can take mixed scrap such as from Ti-6Al-4V and other alloys containing Mo, V and Fe. In addition to flexibility in raw material, it was found that machinability of Ti-54M was superior to Ti-6Al-4V [3]. Ti-54M will save machining costs of parts that require extensive machining. Thus, the better formability and machinability of Ti-54M might be a driving force for replacing Ti-6Al-4V in many aerospace as well as biomedical applications. For these applications, good high-cycle fatigue (HCF) performance is of utmost importance. This can be achieved by microstructural optimization and in particular, by suitable mechanical surface treatments such as SP and BB. In general, these mechanical surface treatments lead to severe plastic deformation and to the development of residual compressive stresses [4, 5]. Residual compressive stresses are well known to enhance the fatigue performance and corrosion resistance by retarding or even suppressing micro-crack growth from the surface into the interior [6, 7]. The present study aims at investigating the influence of various microstructures of Ti-54M on the changes in surface and near-surface properties such as surface topography, micro-hardness-depth and residual stress-depth profiles as induced by SP and BB. The HCF performance after SP and BB of the various microstructures will then be compared to the electropolished baseline (EP).

Experimental Methods

Material was received as square (38 x 38 mm) bar stock in mill-annealed condition. 50 mm long blanks were β-annealed at 1010 °C for 30 min followed by a water-quench (WQ). Blanks were (α+β) uni-directionally rolled at either 800 °C or 900 °C to a deformation degree of φ = 1.2. From the rolled plates, specimen blanks (10 x 10 x 50mm) were taken in transverse direction (TD). The subsequent heat treatments were performed to develop fully lamellar (FL), fully equiaxed (EQ) or duplex (D) microstructures. To generate FL microstructures blanks were beta annealed at 1010°C for 1 hour followed by WQ or air cooling (AC). The EQ microstructures were produced by heating rolled blanks at 800°C for 1 hour followed by WQ or AC. The D microstructures were generated by annealing rolled blanks at 940°C for 1 hour followed by WQ or AC. All material was finally heat treated at 500 °C for 24 hours. Tensile tests were performed using threaded cylindrical specimens having gage lengths and diameters of 25 and 5mm, respectively. Young's moduli were measured with strain gages attached to the gage lengths of the specimens. Initial strain rates were 6.7 x 10^{-4} s^{-1}. HCF tests were performed in rotating beam loading (R = -1) on hour-glass shaped specimens having a minimum diameter of 4mm. All specimens were electrolytically polished (100µm surface removal from as-machined surface) to exclude any machining effects that could mask the results. SP was performed using spherically conditioned cut wire (SCCW14) having an average shot size of 0.36 mm.The Almen intensity was varied from 0.05 to 0.33 mmA. Ball-burnishing was done using a conventional lathe and a hydrostatically driven tool from Ecoroll Company working with a hard metal ball of ∅3mm (HG3). The burnishing pressure was kept constant at 300 bars. The process-induced changes in the surface layer properties were characterized using profilometry, micro-hardness-depth profiles and residual stress-depth profiles. The residual stresses were determined by the incremental hole drilling method. Fatigue crack nucleation sites were studied by optical microscopy and scanning electron microscopy (SEM).

Results and Discussion

The microstructures of the various conditions are shown in Figure 1.

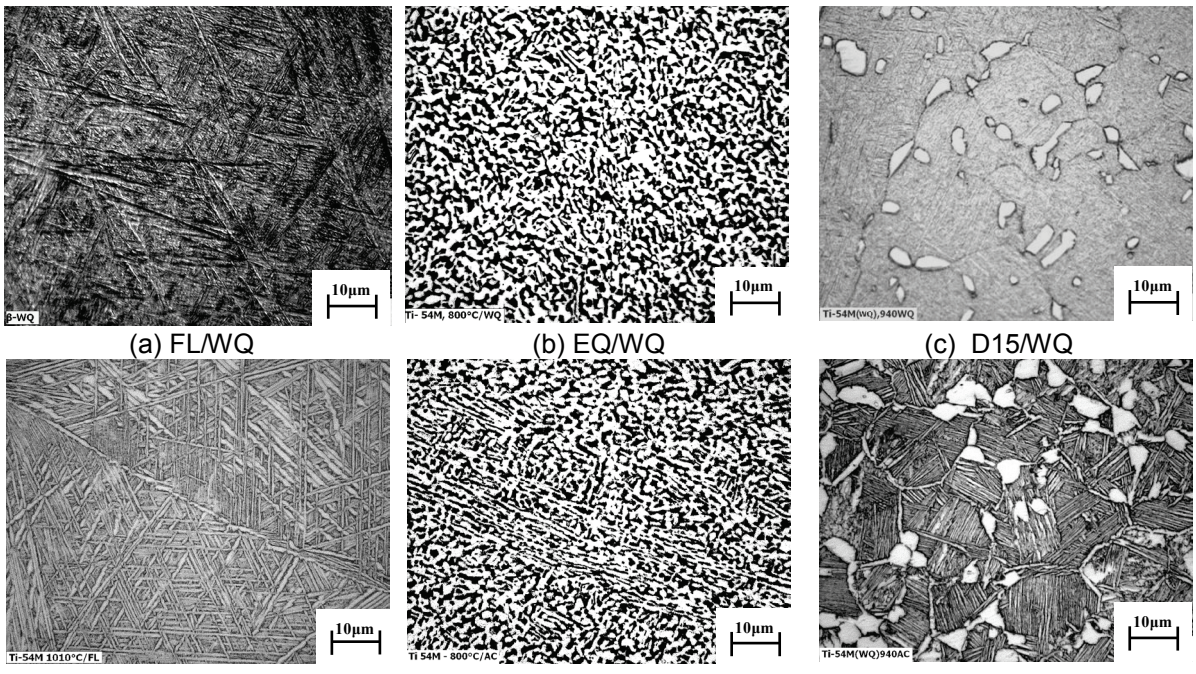

(a) FL/WQ (b) EQ/WQ (c) D15/WQ

(d) FL/AC (e) EQ/AC (f) D15/AC

Figure 1. Microstructures of TIMETAL-54M

FL/WQ exhibits a martensitic microstructure (Fig. 1a). Reducing the cooling rate from WQ to AC, α-plates and thin β-plates are clearly visible indicating a nucleation and growth

controlled forming mechanism in FL/AC (Fig. 1d). EQ/WQ (Fig. 1b) and EQ/AC (Fig. 1e) look very much the same with an average α grain size of 3 µm. D15/WQ (Fig. 1c) and D15/AC (Fig. 1f) are characterized by 15% equiaxed primary α-phase. Similarly as in FL, the matrix microstructure changes from martensitic (D15/WQ, Fig. 1c) to lamellar (D15/AC, Fig. 1f). Tensile properties of the various conditions are illustrated in Table 1.

Table 1. Tensile properties of the various microstructures in Ti-54M

Microstructure	Cooling	YS (MPa)	UTS (MPa)	El (%)	$\varepsilon_F = \ln (A_o/A_F)$
Fully Lamellar (FL)	WQ	1215	1310	1.5	0.06
	AC	1020	1100	8.9	0.15
Equiaxed (EQ)	WQ	1145	1145	12.6	0.62
	AC	1135	1145	15.5	0.72
Duplex (D15)	WQ	1270	1340	8.3	0.34
	AC	1050	1105	14.0	0.50

The cooling rate has a marked effect on the strength properties in FL. Both YS and UTS in FL/WQ are about 200 MPa higher than in FL/AC, this result being caused by the width of the martensite plates (Fig.1a) being much finer than that of the α-lamellae (Fig. 1d). No difference was found in tensile properties between EQ/WQ and EQ/AC (Table 1) which corresponds to the similarity in microstructure (compare Fig. 1b and 1e). The presence of a lamellar matrix in D15 leads to a cooling rate effect on tensile properties very similar to that observed in FL (Table 1). Due to the much smaller former β grain size in D15, ε_F values are highly superior to those in FL. The absence of lamellar portions in EQ and the small α-grain size are the reason for the highest values of ε_F among the various microstructures (Table 1). The influence of Almen intensity in SP on the surface roughness values of EQ/WQ is shown in Figure 2 indicating a linear increase with Almen intensity. The effect of this variation in Almen intensity on the fatigue life at σ_a = 800 MPa is shown in Figure 3. Starting with EP, the fatigue life first increases with an increase in Almen intensity up to about 0.2mmA (Fig. 3) followed by a slight decrease. Thus, 0.20mmA was used for establishing S-N curves.

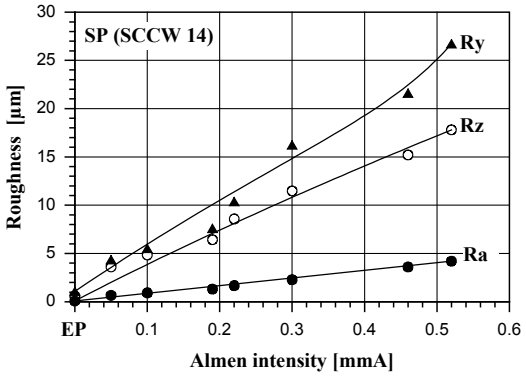

Figure 2. Surface roughness vs. Almen intensity of EQ

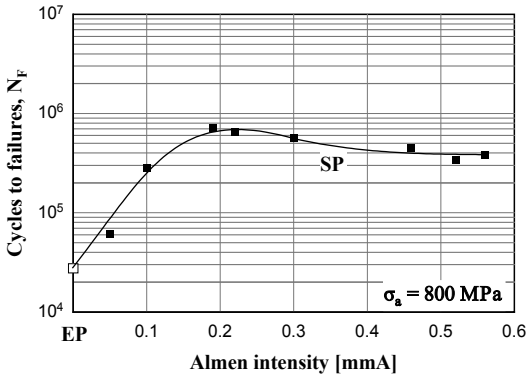

Figure 3. Fatigue life vs. Almen intensity of EQ

The influence of SP with 0.20mmA on the micro-hardness-depth profiles and residual stress-depth profiles of EQ are illustrated in Figure 4 and Figure 5, respectively. In addition, results after BB (300bar) are also plotted. As seen, BB not only leads to a penetration depth of increased hardness markedly higher than in SP (Fig. 4) but also to higher and deeper residual compressive stresses.

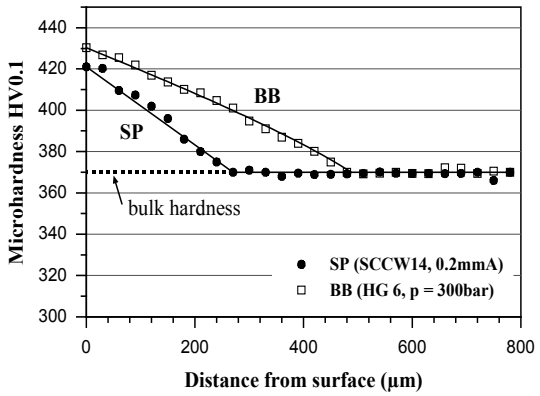

Figure 4. Micro-hardness profiles in EQ

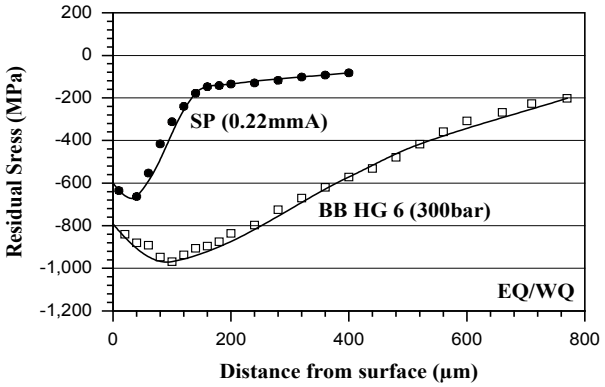

Figure 5. Residual stress profiles in EQ

The S-N curves of the various microstructures are illustrated in Figure 6 comparing SP and BB with EP.

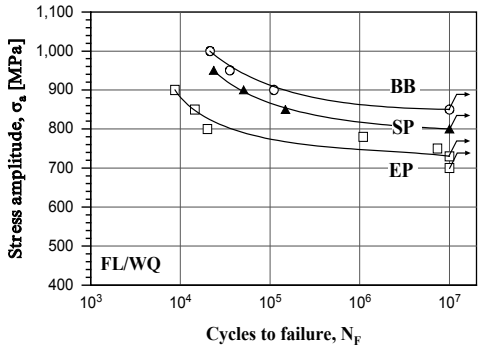

a) FL/WQ

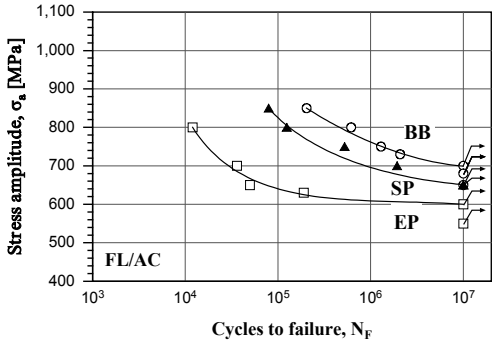

b) FL/AC

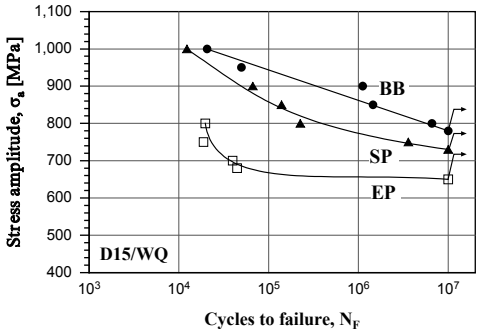

c) D15/WQ

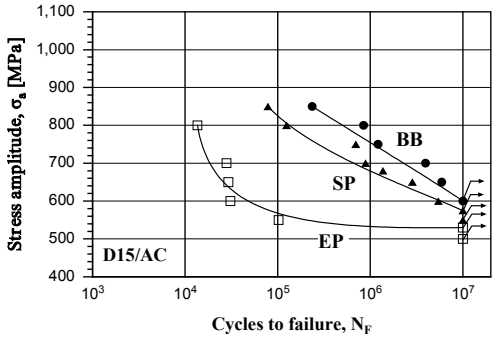

d) D15/AC

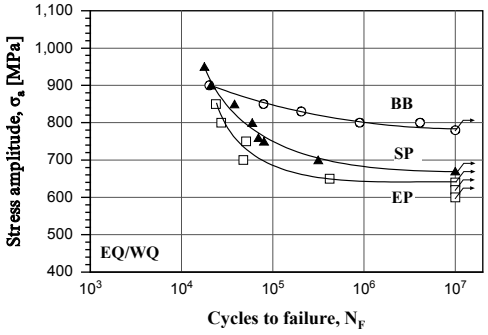

e) EQ/WQ

Figure 6. S-N curves of the various microstructures: effects of SP and BB

The HCF strengths of the various microstructures in EP reflect the corresponding yield stress values (Fig. 7).

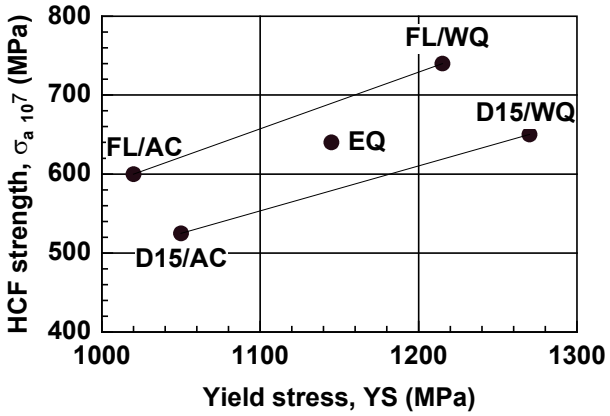

Figure 7. Dependence of HCF strength of baseline EP on yield stress

While the effect of cooling rate on HCF strength is similar between FL and D15, FL results in considerable higher HCF strength values (Fig. 7). From parallel work it is known that HCF cracks in D15/AC nucleate in the (α+β) lamellar matrix indicating that its strength is lower than that of FL [8]. Presumably, this is caused by element partitioning and resulting higher strength of the primary-α-phase in D15. Micro-hardness measurements have shown that the strength of the primary-α-phase opposed to that of the (α+β) lamellar matrix is not affected by cooling rate.

As seen in Figure 6, both SP and BB result in marked enhancements of the HCF strengths of the various microstructures. These data are replotted in Figure 8.

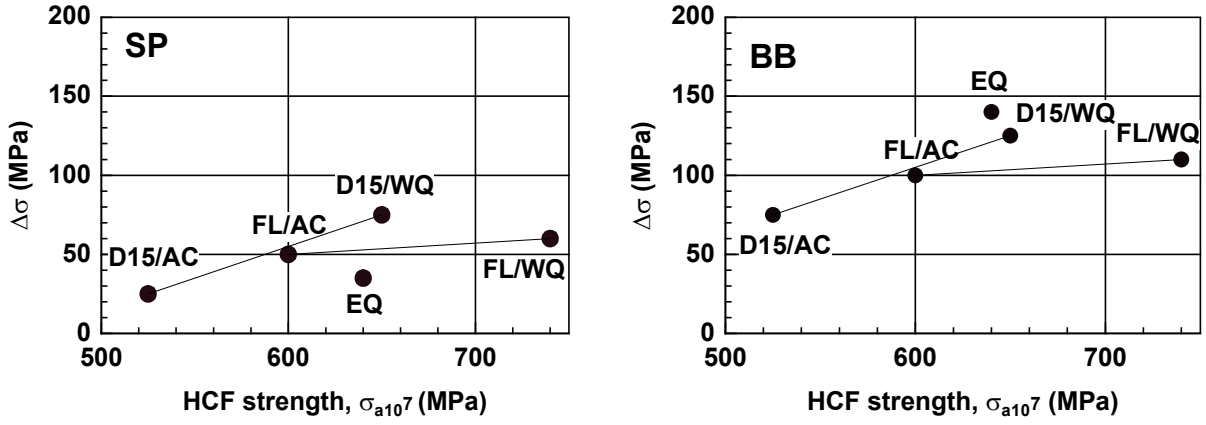

a) SP b) BB

Figure 8. HCF strength improvements

As seen in Figure 8, both SP (Fig. 8a) and BB (Fig. 8b) result in HCF strength improvements which increase with increasing HCF strengths of the baseline EP. Apparently, the degree of improvement depends on the microstructure. Changing the cooling rate from AC to WQ in D15 not only markedly increases the HCF strength from 525 to 650 MPa but also the degree of further improvements by mechanical surface treatments. These amount to 25 and 75 MPa in case of SP for D15/AC and D15/WQ, respectively (Fig. 8a). The corresponding values in case of BB are 75 and 125MPa for D15/AC and D15/WQ, respectively (Fig. 8b). After the same variation in cooling rate, the HCF strength of FL increases from 600 to 740 MPa while further improvements by SP amount to 50 and 60 MPa for FL/AC and FL/WQ, respectively Fig. 8a). The corresponding values in case of BB are 100 and 110 MPa for FL/AC and FL/WQ, respectively (Fig. 8b).

Conclusions

The presented results on well defined microstructures of the new titanium alloy Ti-54M show that YS and HCF strength can be enhanced in FL and D15 microstructures by using a water-quench instead of an air cool from the particular solution temperature. This is clearly related to the refinement of the width of the α-lamellae through martensitic phase transformation in both microstructures. Because of the absence of lamellar components in EQ, no cooling rate effects on microstructure or tensile properties were observed. Mechanical surface treatments SP and BB improve the HCF strength of all tested microstructures. While BB is generally superior to SP, the degree of improvement of the HCF strength depends on both microstructure and strength level.

References

[1] M. Armendia, A. Garay, L. M. Iriarte and P. J. Arrazola, Comparison of the machinablity of Ti6Al4V and TIMETAL 54M using uncoated WC-Co tools, Journal of Materials Processing Technology 210 (2010), pp 197.

[2] V. Venkatesh, Y. Kosaka, J. Fanning, S. Nyakana, Processing and Properties of Timetal 54M, in: Proc. of the 11th Int. World Conference on Titanium (JIMIC5), M. Niinomi, S. Akiyama, M. Ikeda, M. Hagiwara, K. Maruyama (Eds.), Kyoto, Japan,(2007), pp 713.

[3] S. L Nyakana, J. C Fanning, D. W. Tripp, Chemical homogeneity, structure, and properties of Titanium alloys produced by Electron-Beam Single-Melting (EBSM), in: Proc. of the 11th Int. World Conference on Titanium (JIMIC5), M. Niinomi, S. Akiyama, M. Ikeda, M. Hagiwara, K. Maruyama (Eds.), Kyoto, Japan, (2007), pp 749.

[4] J. O. Almen, P. H. Black, Residual stresses and fatigue in metals, McGraw-Hill, New York, 1963.

[5] V. Schulze, Characteristics of surface layers produced by shot peening, in: Proc. of the 8th Int. Conference on Shot Peening, L. Wagner (Eds.), Garmisch-Partenkirchen, Germany, (2002), pp 145.

[6] E. Maawad, H.-G. Brokmeier, M. Hofmann, Ch. Genzel, L. Wagner, Stress distribution in mechanically surface treated Ti-2.5Cu determined by combining energy-dispersive synchrotron and neutron diffraction, Mater. Sci. Eng. A 527 (2010) pp 5745.

[7] L. Wagner, M. Wollmann, Shot peening of non-ferrous alloys to enhance fatigue performance, in: Proc. of the 10th Int. Conference on Shot Peening, K. Tosha (Eds.), Tokyo, Japan, (2008), pp 355.

[8] L. Wagner, K. Zay, M. Wollmann, Y. Kosaka, Thermo-mechanical treatments and mechanical surface treatments on property improvements in the new (α+β) Titanium alloy TIMETAL 54M, PFAM VXIII, Sendai, Japan, (2009) 15-24.